



Late Ediacaran Redox Stability and Metazoan Evolution

Citation

Johnston, David T., S. W. Poulton, T. Goldberg, V. N. Sergeev, V. Podkovyrov, N. G. Vorob'eva, A. Bekker, and Andrew Herbert Knoll. 2012. Late Ediacaran redox stability and metazoan evolution. *Earth and Planetary Science Letters* 335-336:25-35.

Published Version

doi:10.1016/j.epsl.2012.05.010

Permanent link

<http://nrs.harvard.edu/urn-3:HUL.InstRepos:10860657>

Terms of Use

This article was downloaded from Harvard University's DASH repository, and is made available under the terms and conditions applicable to Open Access Policy Articles, as set forth at <http://nrs.harvard.edu/urn-3:HUL.InstRepos:dash.current.terms-of-use#OAP>

Share Your Story

The Harvard community has made this article openly available.
Please share how this access benefits you. [Submit a story](#).

[Accessibility](#)

1 **Late Ediacaran redox stability and metazoan evolution**

2

3 D.T. Johnston¹, S.W. Poulton², T. Goldberg³, V.N. Sergeev⁴, V. Podkovyrov⁵, N.G. Vorob'eva⁴,
4 A. Bekker⁶, A.H. Knoll¹

5 ¹Department of Earth and Planetary Sciences, Harvard University, 20 Oxford St., Cambridge MA 02138

6 ² School of Civil Engineering and Geosciences, Newcastle University, Drummond Building, Newcastle upon Tyne,
7 NE1 7RU, UK

8 Department of Earth Science and Engineering, Imperial College London, London, SW7 2AZ, UK

9 ⁴ Geological Institute, Russian Academy of Sciences, Moscow 109017, Russia

10 ⁵ Institute of Precambrian Geology and Geochronology, Russian Academy of Sciences, St. Petersburg 199034,
11 Russia

12 ⁶ Department of Geological Sciences, University of Manitoba, 125 Dysart Rd., Winnipeg, MB R3T 2N2, Canada

13 corresponding author: (DTJ) johnston@eps.harvard.edu

14 Abstract: 316, Words: 6278, Figures: 7

15

15 **Abstract:** The Neoproterozoic arrival of animals fundamentally changed Earth's biological and
16 geochemical trajectory. Since the early description of Ediacaran and Cambrian animal fossils, a
17 vigorous debate has emerged about the drivers underpinning their seemingly rapid radiation.
18 Some argue for predation and ecology as central to diversification, whereas others point to a
19 changing chemical environment as the trigger. In both cases, questions of timing and feedbacks
20 remain unresolved. Through these debates, the last fifty years of work has largely converged on
21 the concept that a change in atmospheric oxygen levels, perhaps manifested indirectly as an
22 oxygenation of the deep ocean, was causally linked to the initial diversification of large animals.
23 What has largely been absent, but is provided in this study, is a multi-proxy stratigraphic test of
24 this hypothesis. Here, we describe a coupled geochemical and paleontological investigation of
25 Neoproterozoic sedimentary rocks from northern Russia. In detail, we provide iron speciation
26 data, carbon and sulfur isotope compositions, and major element abundances from a
27 predominantly siliciclastic succession (spanning > 1,000 meters) sampled by the Kel'tminskaya-
28 1 drillcore. Our interpretation of these data is consistent with the hypothesis that the pO_2
29 threshold required for diversification of animals with high metabolic oxygen demands was
30 crossed prior to or during the Ediacaran Period. Redox *stabilization* of shallow marine
31 environments was, however, also critical and only occurred about 560 million years ago (Ma),
32 when large motile bilaterians first enter the regional stratigraphic record. In contrast, neither
33 fossils nor geochemistry lend support to the hypothesis that ecological interactions altered the
34 course of evolution in the absence of environmental change. Together, the geochemical and
35 paleontological records suggest a coordinated transition from low oxygen oceans sometime
36 before the Marinoan (~635 Ma) ice age, through better oxygenated but still redox-unstable
37 shelves of the early Ediacaran Period, to the fully and persistently oxygenated marine

38 environments characteristic of later Ediacaran successions that preserve the first bilaterian
39 macrofossils and trace fossils.

40

41 1.0 INTRODUCTION

42 The hypothesis that increased oxygen availability facilitated Ediacaran (635-542 Ma)
43 metazoan evolution dates back more than half a century (Cloud and Drake, 1968; Nursall, 1959).
44 This hypothesis posits that an increase in the oxygen content of shallow-marine environments
45 was physiologically necessary for the emergence of large, highly energetic animals (Raff and
46 Raff, 1970; Rhoads and Morse, 1971). Ecological and physiological observations place lower
47 dissolved oxygen (DO) limits for ocean waters in which different types of animals can live (e.g.,
48 (Diaz and Rosenberg, 1995; Levin, 2003)). They further make predictions about body shape in
49 early animals, based on diffusion length-scales for organisms that lack a circulatory system for
50 bulk oxygen transport (Knoll, 2011; Payne et al., 2011; Raff and Raff, 1970; Runnegar, 1991).
51 Together, then, these physiological requirements for oxygen predict that geochemical evidence
52 for well-oxygenated marine waters should coincide with or slightly antedate fossil records of
53 animals with high oxygen demand.

54 A growing suite of redox-related geochemical tools is now available to test the oxygen-
55 facilitation hypothesis. For instance, reconstructions of the iron and sulfur cycles in Ediacaran
56 strata of Newfoundland suggest a broad consistency between oxygenation and animal
57 diversification (Canfield et al., 2007). There, deep-water axial turbidites with low overall
58 organic carbon contents preserve a shift in the distribution of iron minerals that bespeaks
59 increased DO. This inferred change in redox structure is placed atop the ~580 Ma glacial deposit

60 of the Gaskiers Formation and is followed by the appearance of Ediacaran macrofossils through
61 the overlying Drook, Briscal and Mistaken Point formations. A similar geochemical formula
62 was applied to fossil-bearing sections from South China and the Yukon (McFadden et al., 2008;
63 Narbonne and Aitken, 1990), however the relationship between the fossil record and redox
64 transitions in these basins, especially as they relate to Newfoundland (Canfield et al., 2007), is
65 less clear cut. Correlations among these basins and their stratigraphic successions are
66 challenging, and the postulated role of sulfide as a key toxin in basins developed along the
67 continental margin of the South China craton further complicates physiological interpretations
68 (Li et al., 2010).

69 Thus, the lack of first-order geochemical coherence among these localities, perhaps due
70 in part to locally variable biogeochemical fluxes (Johnston et al., 2010; Kah and Bartley, 2011),
71 means that the direct role that oxygen played in the timing of both local and global animal
72 diversification remains to be fully elucidated. Given this, it is important to acknowledge models
73 of eumetazoan innovation that bypass oxygen entirely and call upon ecology as the primary
74 driver (Butterfield, 2009; Peterson and Butterfield, 2005; Stanley, 1973). In addressing the role
75 of oxygen through the application of robust geochemical techniques, both hypotheses can
76 ultimately be tested.

77 Environmental and ecological hypotheses make distinct predictions about the sequence of
78 biological and geochemical changes, which can be tested through detailed geochemical analyses
79 of fossil-bearing Ediacaran strata. This forms the premise for our current study of Ediacaran
80 marine sediments from the Eastern European Platform (EEP). This succession hosts some of the
81 most exquisite examples of early animal life (Fedonkin et al., 2007; Fedonkin and Waggoner,
82 1997; Martin et al., 2000) and offers a prime opportunity to reconstruct oceanic redox conditions

83 through the application of a range of geochemical methods. Here, we thus revisit both the
84 oxygen facilitation and ecology hypotheses through the application of iron, sulfur, and carbon
85 geochemistry, bulk elemental data, and rigorous statistical analysis.

86

87 2.0 GEOLOGICAL SETTING

88 The Kel'tminskaya-1 drillhole, located near the Dzhezhim–Parma uplift in northern
89 Russia records ~5,000 meters of upper Neoproterozoic and Paleozoic strata that accumulated
90 along the northeast margin of the East European Platform (Fig. 1). The lowermost 2000 m of the
91 core contains a mixed carbonate and siliciclastic succession deposited in a shallow-marine
92 setting, correlated bio- and chemo-stratigraphically to the Cryogenian (850-635 Ma) Karatau
93 Group in the Ural Mountains (Raaben and Oparenkova, 1997; Sergeev, 2006; Sergeev and
94 Seong-Joo, 2006). Age constraints for this part of the succession are limited, but stromatolites,
95 vase-shaped microfossils (Maslov et al., 1994; Porter et al., 2003) and correlation to Pb-Pb dated
96 carbonate rocks of the Min'yar Formation in the Ural Mountains suggest an age of 780 ± 85 Ma
97 (Ovchinnikova et al., 2000).

98 Unconformably overlying Cryogenian strata, and thus separated by > 100 million years,
99 are siliciclastics of the Vycheгда, Redkino and Kotlin formations. The Vycheгда Formation, a
100 600 m thick succession, is dominated by interbedded sandstone, siltstone and shale suggestive of
101 mid-shelf deposition. Diverse large ornamented microfossils first appear low in this unit (at
102 2779 m) and indicate an Ediacaran age (Vorob'eva et al., 2009b) (Fig. 1). No Sturtian or
103 Marinoan-aged diamictites are present in the drillcore, complicating placement of the
104 Cryogenian-Ediacaran boundary. However, typically pre-Ediacaran microfossils occur in mixed

105 coastal siliciclastic rocks in the lowermost six meters of the Vycheгда Formation, suggesting
106 that the period boundary is marked by a cryptic unconformity just above these beds (Vorob'eva
107 et al., 2009a, b).

108 The exact duration of the proposed hiatus is unclear, however overlying Vycheгда shales,
109 interpreted as mid-shelf deposits (Vorob'eva et al., 2009a, b), contain a diverse assemblage of
110 large, highly ornamented organic-walled microfossils akin to the Ediacaran Complex
111 Acanthomorph-dominated Palynoflora (ECAP (Grey, 2005)). In central and southern Australia
112 (Grey and Calver, 2007; Grey et al., 2003), the ECAP assemblage populates a restricted temporal
113 interval, occupying beds that overlie the ca. 580 Ma Acraman impact layer, but underlie the
114 strongly negative C-isotopic excursion of the Wonoka Formation (correlated with the Shuram
115 anomaly in Oman). Well above this interval, diverse Ediacaran macrofossils appear. The same is
116 true in China (Jiang et al., 2007; McFadden et al., 2008), Subhimalayan India (Kaufman et al.,
117 2006), and the Patom region of Siberia (Pokrovskii, 2006; Sergeev et al., 2011). Detrital zircons
118 also constrain ECAP acritarchs in the Hedmark Group, Norway to be younger than 620 \pm 14 Ma
119 (Bingen et al., 2005), consistent with other results. Taken together, these observations most
120 conservatively suggest that the Vycheгда Formation was deposited during the Ediacaran Period,
121 before 558 Ma, a U-Pb constraint provided from the Redkino Formation and discussed below.
122 Given the distribution of ECAP microfossils elsewhere, we suggest that the majority of
123 Vycheгда Formation deposition took place between 580 and 558 Ma.

124 Siliciclastic rocks in the upper 1000 m of the Kel'tminskaya-1 drillhole correlate with the
125 Redkino and Kotlin successions preserved across the EEP (Sokolov and Fedonkin, 1990).
126 Redkino rocks lack highly ornamented microfossils but preserve an exceptional record of
127 Ediacaran macrofossils, including *Kimberella*, widely considered to be the earliest known

128 bilaterian animal (Fedonkin et al., 2007; Fedonkin and Waggoner, 1997) (Fig. 1). Additional
129 information about the paleobiology of Kel'tminskaya-1 core material can be found in (Vorob'eva
130 et al., 2009a, b). U-Pb dates on zircons in Redkino ash beds indicate ages of 555.3 ± 0.3 Ma near
131 the top of the succession (Martin et al., 2000) and 558 ± 1 Ma toward its base (Grazhdankin,
132 2003). Biostratigraphy places the Proterozoic-Cambrian boundary at or near the top of the
133 Kotlin succession.

134

135 3.0 METHODS

136 Iron speciation was performed following a calibrated extraction technique (Poulton and
137 Canfield, 2005). This method targets operationally defined iron pools, such as iron carbonate
138 (Fe_{carb} : ankerite and siderite), Fe^{3+} oxides (Fe_{ox} : goethite and hematite) and mixed valence iron
139 minerals (Fe_{mag} : magnetite). Pyrite iron (Fe_{py}) and sulfur, as well as acid volatile sulfur (AVS;
140 below detection in these samples) were extracted via traditional distillation techniques (Canfield
141 et al., 1986). Together, these pools define a suite of minerals that can be considered
142 biogeochemically available, or highly reactive (FeHr) towards reductive dissolution in surface
143 and near-surface environments ($\text{FeHr} = \text{Fe}_{\text{carb}} + \text{Fe}_{\text{ox}} + \text{Fe}_{\text{mag}} + \text{Fe}_{\text{py}}$) (Poulton et al., 2004a).
144 Total Fe (FeT) additionally comprises a largely unreactive silicate iron pool (FeU), delivered to
145 the marine environment via weathered detrital fluxes (i.e., $\text{FeHr} + \text{FeU} = \text{FeT}$). Both pools are
146 classically defined in relation to their reactivity toward dissolved sulfide (Canfield et al., 1992;
147 Poulton et al., 2004b). Total Fe contents were derived from both HF-HClO₄-HNO₃ extractions
148 and standard XRF analyses. X-ray fluorescence also provided major element chemistry, most

149 notably Al, Ti, K, Na, Si, Mg, Mn, and P (performed at UMass Amherst). All aqueous Fe
150 analyses were performed by AAS, with a RSD of <5% for all stages.

151 Sulfur isotope analyses were performed by combusting sulfide precipitates (see Fe_{py}
152 above) to SO₂ and then run via continuous-flow on a Thermofinnigan Delta V with an analytical
153 reproducibility of 0.2‰, normalized to VCDT. Carbon isotopes were performed on splits of the
154 same bulk sample. Prior to carbon isotope analyses, samples were decalcified with a 10% HCl
155 pre-treatment. Decalcified samples were analyzed for organic carbon isotopes ($\delta^{13}\text{C}_{\text{org}}$) and total
156 organic carbon contents (TOC) via combustion to CO₂ with a Carlo Erba EA interfaced with a
157 Thermofinnigan Delta V configured in continuous flow mode. Samples were run in duplicate
158 with reproducibility of 0.2‰ and <0.05 wt%. Carbonate carbon isotope values ($\delta^{13}\text{C}_{\text{carb}}$) were
159 measured on a Dual Inlet VG Optima gas source mass spectrometer interfaced with an Isocarb
160 prep device. Reproducibility is roughly 0.1‰ and all carbon isotope data are normalized to a
161 VPDB scale.

162

163 4.0 RESULTS AND DISCUSSION

164 We used iron speciation chemistry, major element abundances, and stable carbon and
165 sulfur isotopic ratios to characterize oceanic redox conditions and biogeochemical cycling during
166 deposition of the Kel'tminskaya-1 succession (Fig. 2). The distribution of reactive iron minerals
167 in marine sediment has been calibrated in order to differentiate between oxic and anoxic water
168 column conditions (Canfield et al., 1996; Lyons et al., 2003; Poulton and Canfield, 2011;
169 Raiswell et al., 1988; Raiswell and Canfield, 1996; Raiswell et al., 1994; Raiswell et al., 2001).
170 In keeping with these calibrations, we interpret highly reactive iron (FeHr)/total iron (FeT) >

171 0.38 as diagnostic of anoxia, with Phanerozoic and modern marine Fe_{Hr}/Fe_T values of
172 0.14±0.08 and 0.26±0.08 falling within a range characteristic of an oxic depositional
173 environment (Anderson and Raiswell, 2004; Poulton and Raiswell, 2002; Raiswell and Canfield,
174 1998). Fe/Al provides additional paleoredox information, with the added value of circumventing
175 dilution effects related to carbonate contents (Lyons et al., 2003). In the case of Fe/Al (here Fe
176 refers to Fe_T), crustal values of ~0.5-0.6 commonly characterize oxic conditions, with anoxia
177 generally giving rise to Fe/Al enrichments above this threshold (Lyons and Severmann, 2006).

178 We also report the chemical index of alteration (CIA) for siliciclastic samples in order to
179 monitor the nature and maturity of terrigenous fluxes into the basin (Nesbitt et al., 1997; Nesbitt
180 and Young, 1984; Nesbitt et al., 1996; Tosca et al., 2010). CIA, a measure of the degree of
181 weathering, is expressed as $Al_2O_3/[Al_2O_3 + CaO + Na_2O + K_2O]$. Given the importance of clay
182 minerals in organic matter burial and early diagenetic biogeochemistry (Hedges and Keil, 1995;
183 Keil et al., 1994; Rothman and Forney, 2007), we provide these data to assay potential changes
184 in source terrain for detrital siliciclastics that would in turn effect marine geochemical cycling,
185 all presented against the backdrop of previous work on the Neoproterozoic (Kennedy et al.,
186 2006; Tosca et al., 2010). Finally, reporting on the isotopic composition and abundances of
187 carbon and sulfur allows the geochemical measures described above to be linked more directly to
188 biogeochemical cycling. That is, the stoichiometry of heterotrophic remineralization reactions
189 provides a means of relating organic carbon (and factors associated with production, export and
190 burial) to electron accepting species within the Fe and S cycles (Fe-oxides and sulfate, in
191 particular). Below we discuss the distribution of these data in the context of their specific
192 geological setting, beginning with the oldest, Cryogenian-age samples. The full data are
193 presented in the supplemental materials.

194

195 **4.1 Cryogenian records from the EEP**

196 Geochemical data for the carbonate-rich Cryogenian portion of the Kel'tminkya-1
197 drillhole mirror those of pre-Sturtian successions elsewhere (Canfield et al., 2008; Johnston et
198 al., 2010). Within the lower reach of the drillhole, $\delta^{13}\text{C}_{\text{carb}}$ varies stratigraphically from -4‰ to
199 4‰, consistent with earlier Neoproterozoic values from the Uralian Karatau Group (Podkovyrov
200 et al., 1998) and correlative carbonates on the Siberian Platform (Bartley et al., 2001). Organic
201 carbon content is generally low (< 0.4 wt%), and on average is higher in Cryogenian than in
202 younger intervals of the succession; $\delta^{13}\text{C}_{\text{org}}$ values for carbonate-rich Cryogenian samples vary
203 moderately around a mean of about -29‰. A monotonic $\sim 8\%$ rise in $\delta^{13}\text{C}_{\text{carb}}$ through the
204 Vapol' Formation may suggest an increase in organic carbon burial (Hayes et al., 1999), but a
205 tight, parallel change in $\delta^{13}\text{C}_{\text{org}}$ is lacking. This lack of isotopic covariance is not uncommon in
206 Neoproterozoic carbonates (Fike et al., 2006; Swanson-Hysell et al., 2010), with recent work
207 pointing to complexities associated with $\delta^{13}\text{C}_{\text{org}}$ as masking classic carbon isotope behavior
208 (Johnston et al., 2012; Knoll et al., 1986). In the case of the Cryogenian from Russia, the data
209 reported here support a stratigraphic link to the Ural Mountains and provide yet another example
210 of a pre-Sturtian carbon cycle with a large degree of variability. That is, the biogeochemical
211 picture provided by the Vapol' and Yskemess formations is consistent with those preserved
212 globally.

213 The Vapol' and Yskemess formations are carbonate dominated, with, on average, a
214 weight percent total iron (Fig. 2), much of which occurs as Fe-carbonate. The iron carbonate
215 fraction was determined via the first step of the normal Fe-speciation method, which is a weak

216 acid extract defined to access carbonate phases (ankerite and siderite). The further application of
217 Fe-speciation data requires added discussion. It is important to appreciate that Fe-speciation
218 methods are calibrated on fine-grained siliciclastic sediments and the threshold values that guide
219 the reading of these metrics are similarly rooted. This, of course, complicates the direct and
220 literal interpretation of Fe-speciation data on carbonates. However, a number of points require
221 consideration. Foremost, the determination of iron carbonate, simply as a mass fraction and as
222 presented above, is robust. Next, the logic of Fe speciation methods is based on the precipitation
223 of Fe minerals under anoxic water column conditions and the subsequent settling of these
224 minerals, enriching local sediments. This iron enrichment is only possible when bottom water
225 conditions are anoxic. Thus, iron enrichment should occur in anoxic carbonate-rich
226 environments in the same fashion as it does in siliciclastic sediments, provided that there is a
227 reasonable amount of total Fe to source. Fe enrichment in carbonates can occur because of water
228 column Fe precipitation or suspended load siliciclastic admixture. (Fe/Al ratios for carbonates
229 were not measured due to interferences associated with high $[Ca^{2+}]$, a function of carbonate
230 content.) Nonetheless, where FeT is high, as is the case with the EEP carbonates (FeT averages
231 ~1.3 wt%), the potential for minor Fe mobilization and redistribution following deposition
232 should not result in a spurious redox signal, and its association with carbonates suggests that it is
233 reactive iron as opposed to silicate iron or iron delivered with detrital fluxes. With the
234 discussion above and in noting that Fe in ancient carbonates usually stays close to original
235 depositional values (Tucker and Wright, 1990), Fe speciation has been successfully applied in a
236 variety of siliciclastic-poor settings (e.g. (Goldberg et al., 2005; Kendall et al., 2010; Marz et al.,
237 2008). However, although we argue that the Fe-speciation proxy should generally behave
238 similarly in carbonate-rich and siliciclastic rocks (also see (Poulton and Canfield, 2005)), we do

239 not require the strict interpretation of carbonate iron data for the story forwarded here. We
240 simply present iron data from a limited Cryogenian dataset against the backdrop of
241 contemporaneous siliciclastic units from North America, which is discussed below.

242 Iron speciation data for the Vapol' and Yskemess formations are variable but suggest a
243 highly reactive iron enrichment (and inferred bottom water anoxia), even though most of these
244 rocks were deposited in no more than a few tens of meters of water. Calculated 95% confidence
245 intervals for Fe_{Hr}/Fe_T in the Vapol' and Yskemess are $0.54_{1.21}^{0.04}$ and $0.48_{0.79}^{0.12}$, respectively (see
246 also Fig. 2, 3). For the samples with elevated reactive iron contents, low sulfide contents (Fig. 2)
247 result in low Fe_{py}/Fe_{Hr} ratios (~0.1), which, coupled with an Fe speciation signal that is Fe_{carb}
248 dominated (Figure 3), points to anoxic ferruginous water column conditions (Poulton et al.,
249 2004; Poulton and Canfield, 2011) for nearly 80% of the Cryogenian samples. As noted above,
250 these data simply provide a complementary picture. Interestingly, however, and in support of
251 using Fe methods on carbonates, correlative successions from other continents also feature low
252 pyrite contents and signatures of anoxia. For example, by almost every metric, the EEP results
253 are consistent with the shale-dominated Chuar Group in the Grand Canyon, USA (Johnston et
254 al., 2010). There, a stratigraphically resolved data-set records persistent subsurface water
255 column anoxia, in waters of similar depth, with only modest sulfide production corresponding to
256 intervals of increased TOC burial. Given the dominant role of the atmosphere (and the O₂
257 reservoir) in disseminating oxygen into the surface mixed layer of the ocean, anoxia on the shelf
258 likely reflects lower O₂, noting that local biogeochemistry can influence the DO load (Johnston
259 et al., 2010).

260

261 4.2 Ediacaran records from the EEP

262 Geochemical data from the siliciclastic Ediacaran portion of the Kel'tminskya-1 drillhole
263 (above 2779m) suggest a more fully oxygenated water column, as well as an increasing trend
264 toward redox stability moving upward through the section. Total iron abundances for the
265 Vycheгда, Redkino and Kotlin formations are significantly higher than for the carbonate-rich
266 Cryogenian section, as expected for a shale-dominated succession, with Fe and P concentrations
267 similar to average Phanerozoic shale contents (~5 wt% and 0.07 wt %, respectively; Fig. 2)
268 (Turekian and Wedepohl, 1961). The distribution of reactive iron phases from the EEP suggests
269 a markedly more oxygenated depositional environment for the Ediacaran shales than for the
270 underlying Cryogenian deposits. Ediacaran Fe_{Hr}/Fe_T values oscillate around a mean of $0.26_{0.36}^{0.13}$
271 (95% confidence interval), similar to that characteristic of modern oxic marine sediments (Fig. 2,
272 3) (Poulton and Canfield, 2011; Poulton and Raiswell, 2002).

273 Although suggesting more oxygenated conditions, in detail the chemical variability in the
274 Vycheгда Formation does allow (and may indicate; (Poulton and Canfield, 2011)) recurring
275 intervals of less oxygenated bottom waters, which were replaced by more persistently
276 oxygenated conditions by Redkino time. Along those lines, a closer look at the data reveals an
277 important change *within* the Ediacaran portion of the succession. Notably, the Vycheгда-
278 Redkino sequence boundary separates distinct geochemical regimes (Fig. 2). Thus, we subdivide
279 the Ediacaran stratigraphy into the earlier Ediacaran interval (~580 to 558 Ma) represented by
280 the Vycheгда Formation above 2779m and the upper Ediacaran interval (~558 to 542 Ma)
281 recorded by the Redkino-Kotlin formations. As depicted in Figure 3, many of the reported
282 geochemical metrics from the early and late Ediacaran successions scatter around similar average
283 values, but early Ediacaran samples consistently show more variability. Our data, thus, present a

284 picture of a shelf environment that gradually evolved from one of significant redox heterogeneity
285 in the Cryogenian, through a more oxygenated but still unstable redox regime in the early
286 Ediacaran, to a stable, persistently oxygenated state in the late Ediacaran.

287 In the context of this interpretation, we can consider implications for local
288 biogeochemical cycling. As posited earlier, atmospheric oxygen is one of a few levers on
289 bottom water chemistry, acknowledging that heterotrophy following TOC loading and the
290 ensuing benthic fluxes represent a significant local sink for oxidants (Johnston et al., 2010). To
291 evaluate these contrasting mechanisms, we investigate the relationship between the carbon,
292 phosphorus and iron budgets inferred from Kel'tminskaya-1 samples. The EEP shale is
293 generally TOC lean (Fig. 2, 5), contains typical P contents, and low overall pyrite concentrations.
294 The low observed pyrite contents suggest that dissimilatory sulfate reduction (Canfield, 2001)
295 was not a prominent remineralization pathway in these settings. Without sulfate, this leaves
296 oxygen, nitrate and iron oxides as potentially prominent electron acceptors. The ratio of TOC to
297 reactive iron does not reveal a significant linkage (Fig. 5); however, the conversion of originally
298 mixed valence Fe inputs to predominantly ferrous iron carbonate does require a reductive
299 catalyst, which most naturally would be dissimilatory iron reduction (Fig. 5a). As an extension,
300 the efficiency of P burial relative to organic C can provide important information about
301 preferential P regeneration through remineralization reactions under different redox conditions
302 (Algeo and Ingall, 2007; Ingall and Jahnke, 1994). This often results in a strong positive
303 correlation between C and P, and high organic C:P under anoxic conditions (cf. (Jilbert et al.,
304 2011; Kraal et al., 2010). For example, organic C:P in modern anoxic settings can exceed 300,
305 but deposition under fully oxygenated modern conditions often drive organic C:P below 50
306 (Algeo and Ingall, 2007). In the case of the EEP, organic C:P ratios are consistently low,

307 approaching 1:1 for the Vycheгда and ~2:1 for the Redkino and Kotlin formations (Fig. 5b).
308 Low organic C:P ratios, coupled with low total organic C and the lack of an authigenic P
309 enrichment above that of normal marine shale, is often interpreted as a result of a higher redox
310 potential in the local environment, consistent with an oxygenated water column (Algeo and
311 Ingall, 2007).

312 The distinction between early and late Ediacaran geochemistry can be investigated more
313 quantitatively. To explore the robustness of this partitioning, we bootstrapped a Monte Carlo
314 resampling (n = 1000) of the Vycheгда – Redkino/Kotlin data sets (n = 35 and 44, respectively).
315 This approach clearly identifies differences in Fe/Al ratios and pyrite $\delta^{34}\text{S}$ values, with CIA
316 values holding steady near a value of 0.70 (Fig. 6). Interestingly, the average FeHr/FeT value
317 differs little between lower Ediacaran Vycheгда shales and those of the overlying Redkino-
318 Kotlin succession (Fig. 6a); however, the upper and lower Ediacaran successions differ in the
319 distribution of FeHr/FeT values about the mean, indicating a marked *stabilization* of the redox
320 environment by the late Ediacaran. Whereas the earlier Ediacaran samples record highly
321 variable bottom water conditions, younger Ediacaran shales document a stable and persistently
322 oxic seafloor. This up-section change in FeHr/FeT distribution does not necessarily require an
323 increase in the dissolved oxygen content of seawater, although increasing oxygen provides a
324 ready mechanism for increased redox stability. Fe/Al values also closely track this shift (Fig. 6),
325 and in the absence of apparent change in other possible controls on FeT, these data point toward
326 a broadly oxygenated environment throughout the entire interval of the Ediacaran Period
327 sampled by the drillcore (cf. (Lyons and Severmann, 2006; Lyons et al., 2003; Severmann et al.,
328 2008)). Similarly, more variability in Fe/Al ratios in the early Ediacaran, in part perhaps related
329 to FeT, reflects a greater degree of redox instability, which is again succeeded by stable and

330 oxic-like Fe/Al ratios in the younger Ediacaran part of the succession. Finally, the CIA values of
331 these two populations are similar (Fig. 5), and thus the chemical maturity of terrigenous clay
332 inputs can also be taken as roughly constant, ruling out major change in the terrestrial weathering
333 regime as a driver of the observed geochemical stabilization (Kennedy et al., 2006; Tosca et al.,
334 2010). As clay minerals provide a critical template for the proficient burial of organic matter, it
335 is important to place constraints on this vector. This is especially true considering that the
336 inception of pedogenic clay formation was proposed as a spur for Ediacaran changes in organic
337 burial and associated oxygen production (Kennedy et al., 2006). The absence of a change in the
338 chemical composition of weathered material and sedimentation rate (as reflected by a persistent
339 and similar depositional setting) indicates that there was no major change in provenance or
340 composition of sediments entering the EEP basin.

341 Our data thus indicate that by the time that the main Vychegda sequence began to
342 deposit, marine redox conditions had changed from persistent anoxia to a broadly oxygenated
343 water column. This conclusion, of course, reflects oceanographic conditions in a single basin
344 and does not preclude earlier oxygenation of water masses elsewhere. That noted, data from
345 other continents similarly record a redox transition within the lower part of the Ediacaran Period
346 (Canfield et al., 2007; Fike et al., 2006; Scott et al., 2008; Shen et al., 2008). Where the EEP
347 data extend our understanding is their recording of redox *stabilization*, perhaps at ca. 560 Ma.
348 Neither redox transition nor redox stabilization require that pO_2 reached modern levels in the
349 Ediacaran – indeed, both data and models suggest that present day pO_2 was first reached only in
350 the later Paleozoic Era (Bergman et al., 2004; Berner and Canfield, 1989; Dahl et al., 2010).
351 Rather they suggest that, perhaps for the first time in Earth history, oxygen levels were sufficient
352 to limit the spread of anoxia in shallow water settings.

353

354 **4.3 Insight from the sulfur cycle**

355 The sulfur cycle is sensitive to the oxygen content of the atmosphere, and as such, may
356 provide a test of proposed mid-Ediacaran transitions (cf. (Berner and Canfield, 1989; Claypool et
357 al., 1980; Garrels and Lerman, 1981)). We first look at the limited data from the Cryogenian
358 Vapol' and Yskemess formations. Here, $\delta^{34}\text{S}$ values are highly variable and range from above
359 estimates of contemporaneous seawater sulfate (Johnston et al., 2010) to almost -30‰. Scaling
360 loosely with TOC content (Fig. 7b), the 50‰ range certainly reflects primary microbial
361 contributions from sulfate reduction and may also indicate sulfur disproportionation reactions
362 (Canfield and Teske, 1996; Johnston et al., 2005), although mass-balance effects of local sulfate
363 limitation might also have been in play (Canfield, 2001; Hayes, 2001). Although the data
364 exhibit some scatter, in particular where TOC values are higher, $\delta^{34}\text{S}$ values are generally more
365 enriched, consistent with sulfate limitation within the sediments and, consequently, near-
366 quantitative reduction of pore-water sulfate.

367 The sulfur isotopic composition of pyrite from the Ediacaran portion of the EEP is also
368 quite variable. The $\delta^{34}\text{S}$ values of pyrite within the Vycheгда Formation are, on average, more
369 depleted and variable than sulfides from the overlying Redkino and Kotlin formations (a mean
370 value of 2‰ as opposed to 12‰ for the late Ediacaran; Fig. 6d). Importantly, the Vycheгда
371 Formation is also more pyrite-rich than overlying strata, averaging ~0.08 and ranging up to 0.3
372 wt% pyrite (the Redkino and Kotlin formations average ~0.02 wt%). If we presume a $\delta^{34}\text{S}$ of
373 seawater sulfate between 20‰ and 30‰, similar to estimates from early Ediacaran successions
374 in Oman, Namibia, South China and Australia (Fike et al., 2006; Halverson and Hurtgen, 2007;

375 Hurtgen et al., 2002; Hurtgen et al., 2006; McFadden et al., 2008), then the net fractionation
376 associated with a consortium of microbial metabolisms only requires the influence of sulfate
377 reduction. If the Ediacaran seafloor was moving toward a more oxygenated state, as suggested
378 by iron speciation data, then an oxidative sulfur cycle was almost certainly present in the water
379 column. Emerging tools, specifically the minor sulfur isotopes (Johnston, 2011), may provide a
380 test of this interpretation and allow for the isotopic contributions of reductive and oxidative
381 processes to be more uniquely constrained.

382 The overlying Redkino and Kotlin formations contain much less pyrite and preserve
383 sulfur isotope compositions that cluster toward more enriched values. Although not as enriched
384 as the super-heavy pyrites observed elsewhere (Ries et al., 2009), values are almost always
385 positive ($> 0\text{‰}$). Limited data (Fike and Grotzinger, 2008; Fike et al., 2006; Kampschulte and
386 Strauss, 2004) and a model treatment of that data (Halverson and Hurtgen, 2007) suggest an
387 enrichment in the $\delta^{34}\text{S}$ of seawater sulfate toward the end of the Ediacaran, although more recent
388 datasets suggest seawater sulfate remained near 20‰ at that time (Ries et al., 2009). The lack of
389 consistency among these data is curious, as it points to either the infidelity of certain proxies,
390 poor absolute correlation between continents, or – perhaps most likely – a heterogeneous
391 seawater sulfate reservoir. Regardless of the reason, this variability makes the diagnosis of the
392 Redkino and Kotlin sulfur cycle difficult. If sulfate was becoming more ^{34}S enriched at that
393 time, then the net fractionation between sulfate and sulfide may not have changed significantly
394 from that observed in the underlying Vychegda Formation. However, if sulfate remained largely
395 invariant, these data suggest that the net fractionation decreased drastically. This later scenario
396 could reflect an extreme deficiency in seawater sulfate concentrations (Habicht et al., 2002), but
397 is more likely associated with simple sulfate limitation within the sediments. The latter

398 interpretation is consistent with other geochemical proxies in suggesting that, regionally, anoxia
399 developed only within the sediment column.

400

401 **4.4 Incorporating biological considerations**

402 Geochemistry divides the Kel'tminskaya-1 record into three parts: a pre-Ediacaran
403 (Cryogenian) portion recording the common occurrence of ferruginous water masses in shallow-
404 water environments; a lower Ediacaran succession documenting more oxygenated, but still
405 fluctuating bottom-water conditions on the shelf, and an upper Ediacaran interval that records a
406 fully and persistently oxic water column. Fossils divide regional stratigraphy in much the same
407 fashion (Fig. 1, 2): the Cryogenian rocks are characterized by a modest diversity of protists
408 (Vorob'eva et al., 2009a), recording microscopic eukaryotes that could thrive at low pO_2 . In
409 contrast, the upper Ediacaran (Redkino-Kotlin) succession contains macroscopic animals, as well
410 as trace fossils (Fedonkin et al., 2007; Fedonkin and Waggoner, 1997). In between lie the
411 diverse, large ornamented microfossil assemblage characteristic of lower Ediacaran successions
412 worldwide (Vorob'eva et al., 2009a). Data on morphology, wall ultrastructure, size frequency
413 distribution and preserved intracellular contents suggest that many of these distinctive
414 microfossils represent egg and diapause cysts of early animals (Cohen et al., 2009; Sergeev et al.,
415 2011; Yin et al., 2007). Modern animals produce resting stages when fertilized eggs have a high
416 probability of landing where growth is difficult or impossible (Cohen et al., 2009); therefore, it
417 makes physiological sense that the Ediacaran cysts should be abundant and diverse in basins
418 where geochemical data indicate bottom water redox instability. Whether animal or something
419 else, the abundance of these cysts in Vycheгда Formation shale indicates that environmental

420 conditions were frequently inimical to growth. Few if any of these microfossils persist into beds
421 marked by persistently oxic water column conditions. The hypothesis that the early Ediacaran
422 seafloor was intermediate in redox character to its pre-Ediacaran and late Ediacaran counterparts
423 is also consistent with the presence of moderately differentiated but essentially two-dimensional
424 macrofossils in earlier Ediacaran shales from China (Yuan et al., 2011).

425 Diverse macroscopic animals first appear regionally in Redkino-aged deposits (Sokolov
426 and Fedonkin, 1990; Sokolov and Iwanowski, 1990). Many of these appear to have a simple
427 anatomy, and may largely represent bodyplans in which upper and lower epidermis enclose inert,
428 mesoglea-like material (e.g., (Sperling and Vinther, 2010)). One body-fossil population,
429 however, is widely regarded as the remains of a bilaterian animal. *Kimberella quadrata* was a
430 roughly 2 cm long and at least 1 cm thick organism whose fossil impressions show a distinct
431 anterior-posterior axis with a plane of symmetry running from front to back (Fedonkin et al.,
432 2007). It is occasionally preserved at the end of a trace fossil that documents directional
433 movement across the sediment surface and sometimes also occurs with anterior scratch marks
434 similar to those made by the radulae of mollusks during feeding (Fedonkin et al., 2007). While
435 the precise phylogenetic relationships of *Kimberella* remain open to question, it has a strong
436 claim to status as a bilaterian animal and almost undoubtedly would have required more oxygen
437 for physiological function than other commonly preserved Ediacaran macroorganisms.
438 Independently of *Kimberella*, and consistent with the predictions of molecular clocks (Erwin et
439 al., 2011), trace fossils in the Redkino succession indicate a modest diversity of bilaterian
440 animals. Thus, in the EEP, geochemical evidence for stabilization of pervasively oxic conditions
441 in shelf environments correlates with the appearance of animals with unprecedentedly high
442 oxygen demand.

443 The statistical treatment presented in Figure 6 helps further explain why the Vycheгда
444 and Redkino/Kotlin intervals should be characterized by life cycles with resting stages and large,
445 highly energetic animals, respectively. While neither succession displays Fe-speciation evidence
446 for strong water mass anoxia, and while the mean value of FeHr/FeT is similar for the two
447 intervals, the greater dispersal about the mean for Vycheгда samples results in nearly half of all
448 values falling within the ‘equivocal’ redox range; Redkino/Kotlin samples do not record such a
449 FeHr enrichment. In a recent review, it has been postulated that these intermediate FeHr/FeT
450 values (from 0.26-0.38 in FeHr/FeT) point toward “possible anoxia” (Poulton and Canfield,
451 2011). The term “dysoxia” is commonly frowned upon by geochemists because conditions of
452 low (but measurable) DO are not demarcated by a reliable geochemical fence. Biologists, in
453 contrast, pay close attention to dysoxic/hypoxic waters because their low oxygen contents (less
454 than 1-2 ml/l) strictly limit animal size, locomotion and diversity (e.g., (Diaz and Rosenberg,
455 1995; Seibel and Drazen, 2007; Vaquer-Sunyer and Duarte, 2008)). Hypoxia during the
456 deposition of the Vycheгда Formation may have been sufficiently frequent to favor small
457 animals able to survive episodic bottom water anoxia as well as other unfavorable conditions by
458 forming resting cysts. The removal of this limitation, then, correlates with the first appearance of
459 large, thick, highly motile animals.

460 In combination, then, geochemical and paleontological data from northwestern Russia are
461 fully consistent with the hypothesis that evolving redox conditions exerted a strong influence on
462 the timing of early animal evolution. What about contrasting ecological hypotheses? Few would
463 dispute that ecology played an important role in animal diversification (Butterfield, 2007; Knoll,
464 1994), but what geochemical and paleontological features are uniquely predicted by this
465 hypothesis? The ornamentation of large Ediacaran microfossils have been interpreted as a

466 defensive response to bilaterian predators (Peterson and Butterfield, 2005), but no bilaterian
467 microfossils have been found in Russian or other rocks that contain these ornamented
468 microfossils, and as bilaterians begin to populate the fossil record, the microfossils largely
469 disappear. Geochemically, ecological reorganization in a physiochemically stable ocean should
470 be reflected in changes in biogeochemical cycling across the Vycheгда-Redkino boundary
471 (Butterfield, 2009; Logan et al., 1995). For instance, changes in the articulation of the biological
472 pump (Butterfield, 2009) would carry direct consequences for carbon export, organic matter
473 burial and preservation, and possibly even the type of organic compounds preserved in the
474 sediments. As recorded on the EEP, however, neither TOC nor $\delta^{13}\text{C}_{\text{org}}$ values change
475 significantly across this boundary; nor do pyrite contents or S:C ratios. The sulfur isotopic
476 composition of pyrite does record mid-Ediacaran change (Fig. 2, 6, 7), and, like other proxies,
477 records much less variability in the later Ediacaran. The more positive $\delta^{34}\text{S}$ values found for
478 younger Ediacaran pyrites may simply be another consequence of redox evolution, as sulfate
479 reduction increasingly became restricted to lower and lower horizons within the sediment
480 column, which could have facilitated the net quantitative reduction of pore-water sulfate. The
481 fossil record indicates that evolving animals drove ecological change, especially in the
482 Cambrian, when diverse new bodyplans populated the oceans (Bengston and Morris, 1992);
483 however, available data provide little support for Ediacaran ecological reorganization outside of
484 the context of changing physiochemical conditions.

485

486 5.0 CONCLUSIONS

487 Geochemical reconstructions of Cryogenian and Ediacaran successions on the margin of
488 the Eastern European Platform preserve a history of Earth surface evolution that can be related to
489 similar reconstructions from other continents (Canfield et al., 2007; Johnston et al., 2010;
490 McFadden et al., 2008; Shen et al., 2008), and, more importantly, extends our understanding of
491 how atmospheric oxygen may have influenced the early diversification of metazoans. Previous
492 geochemical models have qualitatively linked proposed increase in the dissolved oxygen content
493 of the ocean with the appearance of macroscopic animals, and although tight constraints on
494 absolute pO_2 remains elusive, data from the EEP suggests that the redox stabilization of the local
495 marine depositional environment may be equally important. This does not preclude a role for
496 changing pO_2 as a means of driving stabilization, although any such mid-Ediacaran change could
497 have been quite modest. A better understanding of absolute pO_2 trajectory may be possible
498 through high-resolution reconstructions of marine depositional environments with high TOC
499 loading (for instance, the Ediacaran successions of the Wernecke and Mackenzie Mountains in
500 the Yukon, Canada), which in contrast to the EEP, would provide a more prominent oxidant sink
501 in the bottom waters and further insight into biogeochemical cycling.

502 In the Kel'tminskaya-1 drillhole, unconformities separate three paleontologically and
503 geochemically defined packages, limiting inferences about the timing, rate, and mechanisms
504 underlying these redox state transitions. That noted, the paleontological progression recorded in
505 northern Russia characterizes Neoproterozoic successions observed globally. The oldest
506 macroscopic animals occur in 565-579 Ma strata from Newfoundland (Narbonne, 2005), a deep-
507 water succession that records a stably oxic seafloor (Canfield et al., 2007) predating Redkino
508 deposition by up to 20 million years. Quite possibly, the fossiliferous Newfoundland rocks
509 record a time interval missing on the EEP along the Vychegda-Redkino sequence boundary. It is

510 also possible, however, that redox stability was not imposed synchronously across the globe
511 (Kah and Bartley, 2011). Indeed, protracted Ediacaran increases in pO_2 might have oxygenated
512 basins regionally, one after another, with biological changes following suit as environmental
513 conditions allowed. This hypothesis can be tested by integrated sequence stratigraphic,
514 paleontological, geochemical, and geochronological analyses of Ediacaran successions.

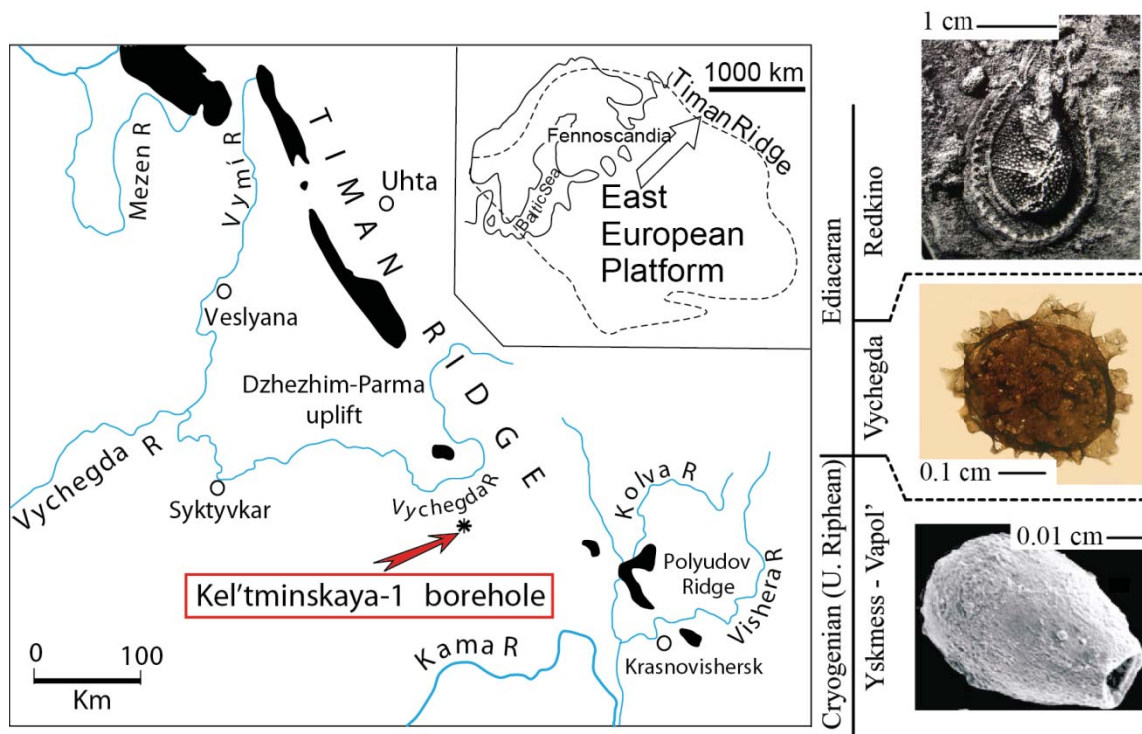
515 By themselves, however, paleontological and geochemical data from the northeastern
516 EEP support two first-order conclusions. First, as evidenced by a growing body of FeHr/FeT
517 data, the oft-cited Neoproterozoic ‘oxygenation’ does not appear to be associated with the
518 Shuram anomaly, as iron speciation data suggests an earlier arrival of this oxidizing capacity and
519 cannot speak to the rate of change (gradual versus abrupt). Continued study of Cryogenian
520 records will help to identify and describe the anatomy of this oxygenation, were a profound
521 change in atmospheric chemistry to exist. Whatever the answer, the participation of oxygen in
522 the atmospheric carbon cycle (as it interacts with critical greenhouse gasses, namely CO_2 and
523 CH_4) suggests a relationship between Neoproterozoic pO_2 and low-latitude Cryogenian
524 glaciations (Hoffman et al., 1998). Second, and most important for biological records, by about
525 580-560 Ma, redox stability came to define shallow marine seafloor environments, possibly (but
526 not necessarily) reflecting a further increase in pO_2 . Our data thus most closely support the
527 classic hypothesis that increasing atmospheric oxygen paved the way for the global expansion of
528 bilaterian macrofossils, but underscores the role of redox *stability* in potentiating end-Proterozoic
529 evolutionary events.

530

531 **Acknowledgements:** We appreciate early and ongoing discussions with P. Cohen, N. Tosca, B.
532 Gill and E. Sperling. D. Schrag and G. Eiseid are thanked for laboratory assistance. This
533 work was funded by the Harvard Microbial Sciences Initiative (DTJ), NASA Exobiology (DTJ,
534 AHK) and the Astrobiology Institute, MIT node (DJ and AHK), NERC (SWP), RBBR grant 10-
535 05-00294 (VNS and NGV), and NSERC Discovery (AB).

536

536 **Figure 1:** A map of the Timan Ridge area showing the location of the Kel'tminskaya-1 drillhole
 537 on the northeastern margin of the Eastern European Platform (see arrow on the inset for the
 538 location on the Eastern European Platform). At right, a cartoon timeline of the characteristic
 539 fossils found in Cryogenian and Ediacaran rocks; protistan assemblages (Porter et al., 2003) are
 540 replaced by large ornamented microfossils, which gave way to complex animals (e.g.
 541 *Kimberella*).



542

543

543 **Figure 2:** Stratigraphic redox proxy variations for the Kel'tminskaya-1 drillhole. Note the break
 544 in vertical scale at the Vapol'–Vycheгда sequence boundary. The age of deposition is based on
 545 lithological and biostratigraphic correlation to the White Sea and Ural Mountains successions.
 546 Note that the 635 Ma age relates to the strata underlying the hiatus in the lower Vycheгда,
 547 whereas the ~580 Ma age relates to that of the overlying ECAP-containing portion of the unit.
 548 All methods and additional data are described in the text and presented in the supplemental
 549 materials. The two leftmost chemostratigraphic frames are on a log scale. Vertical lines in the
 550 FeHr/FeT column are discussed in the text, with red circles with lines extending horizontally
 551 representing samples with FeHr/FeT > 0.6 and indicate anoxia. Where indicating anoxia, all
 552 samples are ferruginous. Carbon isotope axes for carbonate and organic carbon (far right panel)
 553 are offset by 31‰.

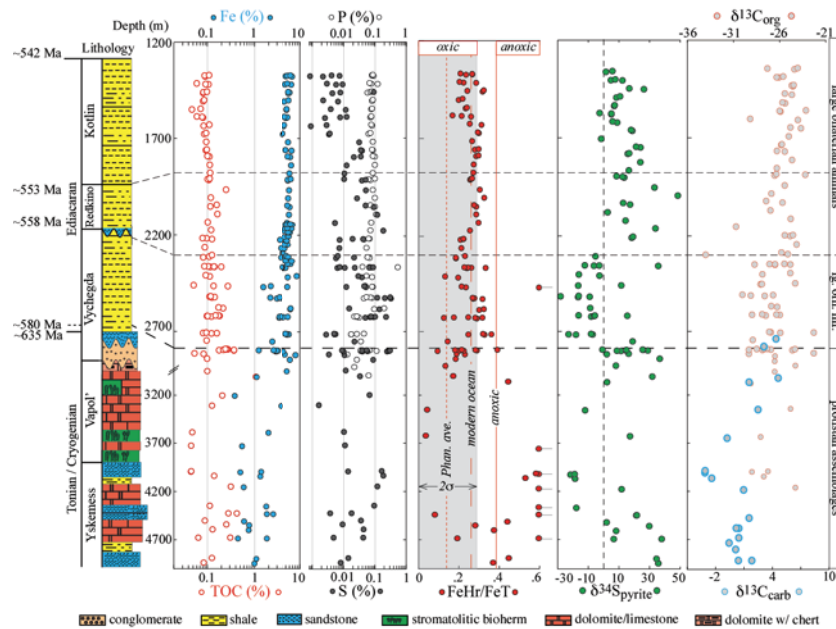
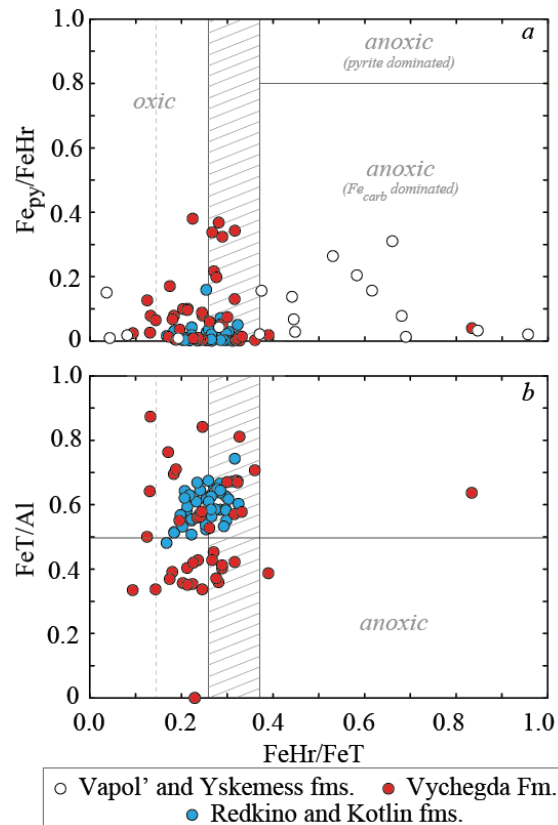


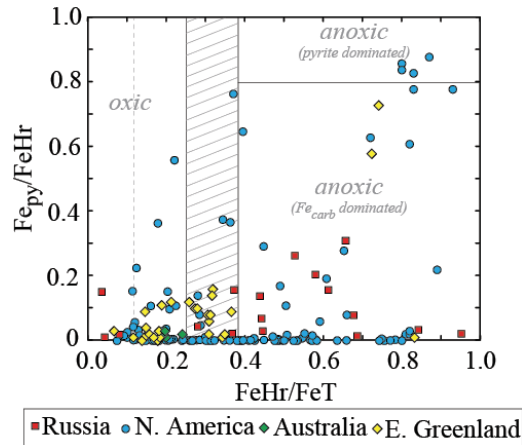
Figure 2

555 **Figure 3:** Two frames indicating the relationship between FeHr/FeT (a measure of anoxia)
 556 versus **(a)** top: a quantification of pyrite iron, Fe_{py}/FeHr and **(b)** bottom: an alternative means of
 557 recording anoxia. A key to the symbols is listed under the figure, with all data coming from this
 558 work. In **(a)**, regions of the plot characteristic of particular water column redox state and
 559 chemistry are noted. That is, FeHr/FeT > 0.38 is indicative of anoxia, whereas values below the
 560 modern average (0.26) are indicative of oxic conditions (Anderson and Raiswell, 2004; Poulton
 561 and Canfield, 2011; Poulton and Raiswell, 2002; Raiswell and Canfield, 1998). The hashed
 562 region, between these two values, carries a more equivocal meaning. For reference, the
 563 Phanerozoic average for shale is also listed (dashed line). In frame **(b)**, the crustal average of
 564 Fe/Al is indicated. See text for further discussions, especially that of the Vapol' and Yskemess
 565 formation carbonates.



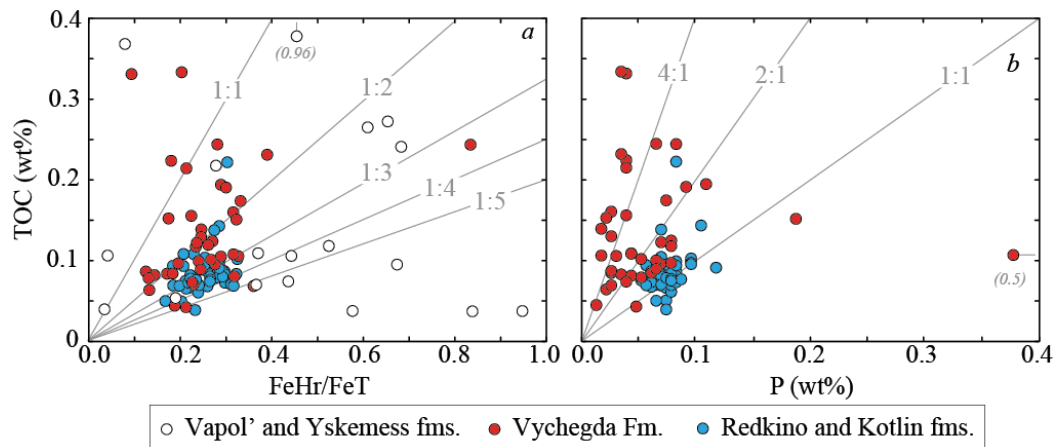
566

567 **Figure 4:** A summary of Fe-speciation data for pre-Sturtian sediments from Russia (this work),
 568 North America (Johnston et al., 2010), East Greenland, and Australia (Canfield et al., 2008).
 569 Axes are the same as Figure 3a, as are distinctions in FeHr/FeT.



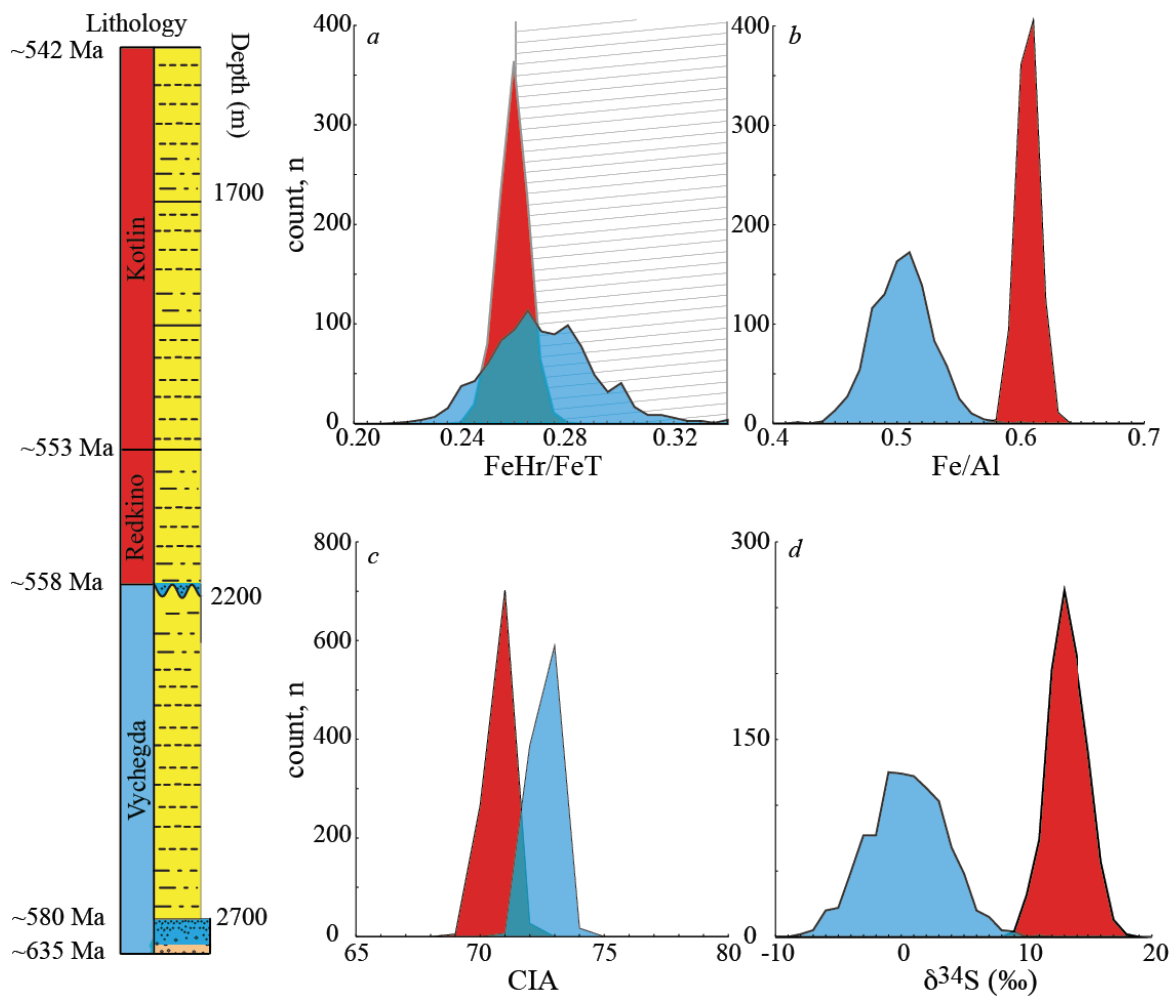
570

571 **Figure 5:** An analysis of the covariance between different biogeochemical metrics. Here, we
 572 examine changes in TOC against (a) reactive iron to total iron ratios, and (b) versus total P
 573 content. Both figures are also contoured by lines representing different ratios between the
 574 abscissa and ordinate measures. These features are fully described in the text and both relate to
 575 oxygen content of the local environment.



576

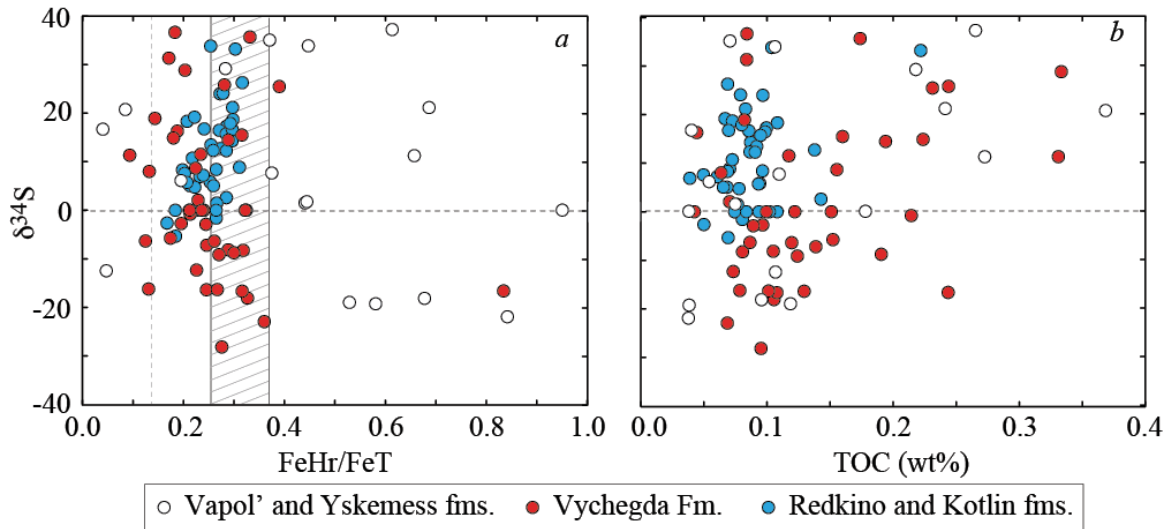
577 **Figure 6:** A statistical resampling of key geochemical metrics from the Ediacaran of the EEP.
 578 Data sets were divided at the Vycheгда-Redkino sequence boundary (Vycheгда in blue,
 579 Redkino and Kotlin in red). Importantly, sampling of the Vycheгда began at 2779 m, the bed at
 580 which distinctly Ediacaran acritarchs first appear (Vorob'eva et al., 2009a). **a)** A measure of
 581 overall water column redox, FeHr/FeT. **b)** The relationship between Fe and Al. **c)** The chemical
 582 index of alteration is described in the text. **d)** The isotopic composition of pyrite sulfur. In all
 583 cases, one thousand synthetic runs were performed (binned and recorded on ordinate axis).
 584 Ordinate axis scale changes from frame to frame.



585

586

586 **Figure 7:** Two plots examining the relationship between the sulfur isotopic composition of
587 pyrite and **(a)** reactive to total iron ratio (FeHr/FeT) and **(b)** total organic carbon content, TOC.
588 Symbols are described below the figure, and the data is discussed in the text.



590 REFERENCE LIST:

- 591 Algeo, T.J., Ingall, E., 2007. Sedimentary C_{org} : P ratios, paleocean ventilation, and
592 Phanerozoic atmospheric pO_2 . *Palaeogeography Palaeoclimatology Palaeoecology* 256,
593 130-155.
- 594 Anderson, T.F., Raiswell, R., 2004. Sources and mechanisms for the enrichment of highly
595 reactive iron in euxinic Black Sea sediments. *American Journal of Science* 304, 203-233.
- 596 Bartley, J.K., Semikhatov, M.A., Kaufman, A.J., Knoll, A.H., Pope, M.C., Jacobsen, S.B., 2001.
597 Global events across the Mesoproterozoic-Neoproterozoic boundary: C and Sr isotopic
598 evidence from Siberia. *Precambrian Research* 111, 165-202.
- 599 Bengtson, S., Morris, S.C., 1992. Early radiation of biomineralizing phyla. *Topics in*
600 *Geobiology* 10, 447-481.
- 601 Bergman, N.M., Lenton, T.M., Watson, A.J., 2004. COPSE: A new model of biogeochemical
602 cycling over Phanerozoic time. *American Journal of Science* 304, 397-437.
- 603 Berner, R.A., Canfield, D.E., 1989. A new model for atmospheric oxygen over Phanerozoic
604 time. *American Journal of Science* 289, 333-361.
- 605 Bingen, B., Griffin, W.L., Torsvik, T.H., Saeed, A., 2005. Timing of Late Neoproterozoic
606 glaciation on Baltica constrained by detrital zircon geochronology in the Hedmark Group,
607 south-east Norway. *Terra Nova* 17, 250-258.
- 608 Butterfield, N.J., 2007. Macroevolution and macroecology through deep time. *Palaeontology*
609 50, 41-55.
- 610 Butterfield, N.J., 2009. Oxygen, animals and oceanic ventilation: an alternative view.
611 *Geobiology* 7, 1-7.

- 612 Canfield, D.E., 2001. Biogeochemistry of sulfur isotopes, *Stable Isotope Geochemistry*, pp.
613 607-636.
- 614 Canfield, D.E., Lyons, T.W., Raiswell, R., 1996. A model for iron deposition to euxinic Black
615 Sea sediments. *American Journal of Science* 296, 818-834.
- 616 Canfield, D.E., Poulton, S.W., Knoll, A.H., Narbonne, G.M., Ross, G., Goldberg, T., Strauss, H.,
617 2008. Ferruginous conditions dominated later neoproterozoic deep-water chemistry.
618 *Science* 321, 949-952.
- 619 Canfield, D.E., Poulton, S.W., Narbonne, G.M., 2007. Late-Neoproterozoic deep-ocean
620 oxygenation and the rise of animal life. *Science* 315, 92-95.
- 621 Canfield, D.E., Raiswell, R., Bottrell, S., 1992. The reactivity of sedimentary iron minerals
622 towards sulfide. *American Journal of Science* 292, 659-683.
- 623 Canfield, D.E., Raiswell, R., Westrich, J.T., Reaves, C.M., Berner, R.A., 1986. The use of
624 chromium reduction in the analysis of reduced inorganic sulfur in sediments and shales.
625 *Chemical Geology* 54, 149-155.
- 626 Canfield, D.E., Teske, A., 1996. Late Proterozoic rise in atmospheric oxygen concentration
627 inferred from phylogenetic and sulphur-isotope studies. *Nature* 382, 127-132.
- 628 Claypool, G.E., Holser, W.T., Kaplan, I.R., Sakai, H., Zak, I., 1980. The age curves of sulfur and
629 oxygen isotopes in marine sulfate and their mutual interpretation. *Chemical Geology* 28,
630 199-260.
- 631 Cloud, P.E., Drake, E.T., 1968. Pre-metazoan evolution and the origins of the Metazoa.
632 *Evolution and environment: a symposium.*, 1-72.

- 633 Cohen, P.A., Knoll, A.H., Kodner, R.B., 2009. Large spinose microfossils in Ediacaran rocks as
634 resting stages of early animals. *Proceedings of the National Academy of Sciences of the*
635 *United States of America* 106, 6519-6524.
- 636 Dahl, T.W., Hammarlund, E.U., Anbar, A.D., Bond, D.P.G., Gill, B.C., Gordon, G.W., Knoll, A.H.,
637 Nielsen, A.T., Schovsbo, N.H., Canfield, D.E., 2010. Devonian rise in atmospheric oxygen
638 correlated to the radiations of terrestrial plants and large predatory fish. *Proceedings of the*
639 *National Academy of Sciences of the United States of America* 107, 17911-17915.
- 640 Diaz, R.J., Rosenberg, R., 1995. Marine benthic hypoxia: A review of its ecological effects and
641 the behavioural responses of benthic macrofauna, in: Ansell, A.D., Gibson, R.N., Barnes, M.
642 (Eds.), *Oceanography and Marine Biology - an Annual Review*, Vol 33, pp. 245-303.
- 643 Erwin, D.H., Laflamme, M., Tweedt, S.M., Sperling, E.A., Pisani, D., Peterson, K.J., 2011. The
644 Cambrian Conundrum: Early Divergence and Later Ecological Success in the Early History
645 of Animals. *Science* 334, 1091-1097.
- 646 Fedonkin, M., Simonetta, A., Ivantsov, A.Y., 2007. New data on *Kimberella*, the Vendian
647 mollusc-like organism (White Sea region, Russia): palaeoecological and evolutionary
648 implications. *Geological Society Special Publication* 286, 157-179.
- 649 Fedonkin, M.A., Waggoner, B.M., 1997. The Late Precambrian fossil *Kimberella* is a mollusc-
650 like bilaterian organism. *Nature* 388, 868-871.
- 651 Fike, D.A., Grotzinger, J.P., 2008. A paired sulfate-pyrite $\delta^{34}\text{S}$ approach to understanding the
652 evolution of the Ediacaran-Cambrian sulfur cycle. *Geochimica Et Cosmochimica Acta* 72,
653 2636-2648.
- 654 Fike, D.A., Grotzinger, J.P., Pratt, L.M., Summons, R.E., 2006. Oxidation of the Ediacaran
655 Ocean. *Nature* 444, 744-747.

- 656 Garrels, R.M., Lerman, A., 1981. Phanerozoic cycles of sedimentary carbon and sulfur.
657 Proceedings of the National Academy of Sciences of the United States of America-Physical
658 Sciences 78, 4652-4656.
- 659 Goldberg, T., Poulton, S.W., Strauss, H., 2005. Sulphur and oxygen isotope signatures of late
660 Neoproterozoic to early Cambrian sulphate, Yangtze Platform, China: Diagenetic
661 constraints and seawater evolution. Precambrian Research 137, 223-241.
- 662 Grazhdankin, D.V., 2003. Structure and depositional environment of the Vendian Complex
663 in the southeastern White Sea area. Stratigraphy and Geological Correlation 11, 313-331.
- 664 Grey, K., 2005. Ediacaran palynology of Australia. Memoirs of the Association of
665 Australasian Palaeontologists 31, 1-439.
- 666 Grey, K., Calver, C.R., 2007. Correlating the Ediacaran of Australia. Geological Society Special
667 Publication 286, 115-135.
- 668 Grey, K., Walter, M.R., Calver, C.R., 2003. Neoproterozoic biotic diversification: Snowball
669 Earth or aftermath of the Acraman impact? Geology 31, 459-462.
- 670 Habicht, K.S., Gade, M., Thamdrup, B., Berg, P., Canfield, D.E., 2002. Calibration of sulfate
671 levels in the Archean Ocean. Science 298, 2372-2374.
- 672 Halverson, G.P., Hurtgen, M.T., 2007. Ediacaran growth of the marine sulfate reservoir.
673 Earth and Planetary Science Letters 263, 32-44.
- 674 Hayes, J.M., 2001. Fractionation of carbon and hydrogen isotopes in biosynthetic processes,
675 Stable Isotope Geochemistry, pp. 225-277.
- 676 Hayes, J.M., Strauss, H., Kaufman, A.J., 1999. The abundance of ^{13}C in marine organic matter
677 and isotopic fractionation in the global biogeochemical cycle of carbon during the past 800
678 Ma. Chemical Geology 161, 103-125.

- 679 Hedges, J.I., Keil, R.G., 1995. Sedimentary organic matter preservation - an assessment and
680 speculative synthesis. *Marine Chemistry* 49, 81-115.
- 681 Hoffman, P.F., Kaufman, A.J., Halverson, G.P., Schrag, D.P., 1998. A Neoproterozoic snowball
682 earth. *Science* 281, 1342-1346.
- 683 Hurtgen, M.T., Arthur, M.A., Suits, N.S., Kaufman, A.J., 2002. The sulfur isotopic composition
684 of Neoproterozoic seawater sulfate: implications for a snowball Earth? *Earth and Planetary
685 Science Letters* 203, 413-429.
- 686 Hurtgen, M.T., Halverson, G.P., Arthur, M.A., Hoffman, P.F., 2006. Sulfur cycling in the
687 aftermath of a 635-Ma snowball glaciation: Evidence for a syn-glacial sulfidic deep ocean.
688 *Earth and Planetary Science Letters* 245, 551-570.
- 689 Ingall, E., Jahnke, R., 1994. Evidence for enhanced phosphorus regeneration from marine
690 sediments overlain by oxygen depleted waters. *Geochimica Et Cosmochimica Acta* 58,
691 2571-2575.
- 692 Jiang, G., Kaufman, A.J., Christie-Blick, N., Zhang, S., Wu, H., 2007. Carbon isotope variability
693 across the Ediacaran Yangtze platform in South China: Implications for a large surface-to-
694 deep ocean delta C-13 gradient. *Earth and Planetary Science Letters* 261, 303-320.
- 695 Jilbert, T., Slomp, C.P., Gustafsson, B.G., Boer, W., 2011. Beyond the Fe-P-redox connection:
696 preferential regeneration of phosphorus from organic matter as a key control on Baltic Sea
697 nutrient cycles. *Biogeosciences* 8, 1699-1720.
- 698 Johnston, D.T., 2011. Multiple sulfur isotopes and the evolution of Earth's surface sulfur
699 cycle. *Earth-Science Reviews* 106, 161-183.
- 700 Johnston, D.T., Macdonald, F.A., Gill, B.C., Hoffman, P.F., Schrag, D.P., 2012. Uncovering the
701 Neoproterozoic carbon cycle. *Nature* 483, 320-U110.

- 702 Johnston, D.T., Poulton, S.W., Dehler, C., Porter, S., Husson, J., Canfield, D.E., Knoll, A.H., 2010.
703 An emerging picture of Neoproterozoic ocean chemistry: Insights from the Chuar Group,
704 Grand Canyon, USA. *Earth and Planetary Science Letters* 290, 64-73.
- 705 Johnston, D.T., Wing, B.A., Farquhar, J., Kaufman, A.J., Strauss, H., Lyons, T.W., Kah, L.C.,
706 Canfield, D.E., 2005. Active microbial sulfur disproportionation in the Mesoproterozoic.
707 *Science* 310, 1477-1479.
- 708 Kah, L.C., Bartley, J.K., 2011. Protracted oxygenation of the Proterozoic biosphere.
709 *International Geology Review* 53, 1424-1442.
- 710 Kampschulte, A., Strauss, H., 2004. The sulfur isotopic evolution of Phanerozoic seawater
711 based on the analysis of structurally substituted sulfate in carbonates. *Chemical Geology*
712 204, 255-286.
- 713 Kaufman, A.J., Jiang, G.Q., Christie-Blick, N., Banerjee, D.M., Rai, V., 2006. Stable isotope
714 record of the terminal Neoproterozoic Krol platform in the Lesser Himalayas of northern
715 India. *Precambrian Research* 147, 156-185.
- 716 Keil, R.G., Montlucon, D.B., Prahl, F.G., Hedges, J.I., 1994. Sorptive preservation of labile
717 organic matter in marine sediments. *Nature* 370, 549-552.
- 718 Kendall, B., Reinhard, C.T., Lyons, T., Kaufman, A.J., Poulton, S.W., Anbar, A.D., 2010.
719 Pervasive oxygenation along late Archaean ocean margins. *Nature Geoscience* 3, 647-652.
- 720 Kennedy, M., Droser, M., Mayer, L.M., Pevear, D., Mrofka, D., 2006. Late Precambrian
721 oxygenation; Inception of the clay mineral factory. *Science* 311, 1446-1449.
- 722 Knoll, A.H., 1994. Proterozoic and early Cambrian protists - evidence for accelerating
723 evolutionary tempo. *Proceedings of the National Academy of Sciences of the United States*
724 *of America* 91, 6743-6750.

- 725 Knoll, A.H., 2011. The Multiple Origins of Complex Multicellularity, in: Jeanloz, R.F.K.H.
726 (Ed.), *Annual Review of Earth and Planetary Sciences*, Vol 39, pp. 217-239.
- 727 Knoll, A.H., Hayes, J.M., Kaufman, A.J., Swett, K., Lambert, I.B., 1986. Secular variation in
728 carbon isotope ratios from upper Proterozoic successions of Svalbard and east Greenland.
729 *Nature* 321, 832-838.
- 730 Kraal, P., Slomp, C.P., de Lange, G.J., 2010. Sedimentary organic carbon to phosphorus ratios
731 as a redox proxy in Quaternary records from the Mediterranean. *Chemical Geology* 277,
732 167-177.
- 733 Levin, L.A., 2003. Oxygen minimum zone benthos: Adaptation and community response to
734 hypoxia. *Oceanography and Marine Biology*, Vol 41 41, 1-45.
- 735 Li, C., Love, G.D., Lyons, T.W., Fike, D.A., Sessions, A.L., Chu, X.L., 2010. A Stratified Redox
736 Model for the Ediacaran Ocean. *Science* 328, 80-83.
- 737 Logan, G.A., Hayes, J.M., Hieshima, G.B., Summons, R.E., 1995. Terminal Proterozoic
738 reorganization of biogeochemical cycles. *Nature* 376, 53-56.
- 739 Lyons, T.W., Severmann, S., 2006. A critical look at iron paleoredox proxies: New insights
740 from modern euxinic marine basins. *Geochimica Et Cosmochimica Acta* 70, 5698-5722.
- 741 Lyons, T.W., Werne, J.P., Hollander, D.J., Murray, R.W., 2003. Contrasting sulfur
742 geochemistry and Fe/Al and Mo/Al ratios across the last oxic-to-anoxic transition in the
743 Cariaco Basin, Venezuela. *Chemical Geology* 195, 131-157.
- 744 Martin, M.W., Grazhdankin, D.V., Bowring, S.A., Evans, D.A.D., Fedonkin, M.A., Kirschvink,
745 J.L., 2000. Age of Neoproterozoic bilaterian body and trace fossils, White Sea, Russia:
746 Implications for metazoan evolution. *Science* 288, 841-845.

- 747 Marz, C., Poulton, S.W., Beckmann, B., Kuster, K., Wagner, T., Kasten, S., 2008. Redox
748 sensitivity of P cycling during marine black shale formation: Dynamics of sulfidic and
749 anoxic, non-sulfidic bottom waters. *Geochimica Et Cosmochimica Acta* 72, 3703-3717.
- 750 Maslov, A., ZM, A., LA, K., VN, P., 1994. First finds of melancyrilliums in Riphean type
751 section, southern Ural Mountains, The results, problems and perspectives of the
752 Precambrian deposits, areas, geological mapping on the territory of Russia, p. 90.
- 753 McFadden, K.A., Huang, J., Chu, X.L., Jiang, G.Q., Kaufman, A.J., Zhou, C.M., Yuan, X.L., Xiao,
754 S.H., 2008. Pulsed oxidation and biological evolution in the Ediacaran Doushantuo
755 Formation. *Proceedings of the National Academy of Sciences of the United States of*
756 *America* 105, 3197-3202.
- 757 Narbonne, G.M., 2005. The ediacarabiota: Neoproterozoic origin of animals and their
758 ecosystems. *Annual Review of Earth and Planetary Sciences* 33, 421-442.
- 759 Narbonne, G.M., Aitken, J.D., 1990. Ediacaran fossils from the Sekwi Brook area, Mackenzie
760 Mountains, northwest Canada. *Palaeontology* 33, 945-980.
- 761 Nesbitt, H.W., Fedo, C.M., Young, G.M., 1997. Quartz and feldspar stability, steady and non-
762 steady-state weathering, and petrogenesis of siliciclastic sands and muds. *Journal of*
763 *Geology* 105, 173-191.
- 764 Nesbitt, H.W., Young, G.M., 1984. Predictions of some weathering trends of plutonic and
765 volcanic rocks based on thermodynamic and kinetic considerations. *Geochimica Et*
766 *Cosmochimica Acta* 48, 1523-1534.
- 767 Nesbitt, H.W., Young, G.M., McLennan, S.M., Keays, R.R., 1996. Effects of chemical
768 weathering and sorting on the petrogenesis of siliciclastic sediments, with implications for
769 provenance studies. *Journal of Geology* 104, 525-542.

- 770 Nursall, J.R., 1959. Oxygen as a prerequisite to the origin of the Metazoa. *Nature* 183, 1170-
771 1172.
- 772 Ovchinnikova, G.V., Vasil'eva, I.M., Semikhatov, M.A., Gorokhov, I.M., Kuznetsov, A.B.,
773 Gorokhovskii, B.M., Levskii, L.K., 2000. The Pb-Pb trail dating of carbonates with open U-Pb
774 systems: The Min'yar Formation of the Upper Riphean stratotype, southern Urals.
775 *Stratigraphy and Geological Correlation* 8, 529-543.
- 776 Payne, J.L., McClain, C.R., Boyer, A.G., Brown, J.H., Finnegan, S., Kowalewski, M., Krause, R.A.,
777 Lyons, S.K., McShea, D.W., Novack-Gottshall, P.M., Smith, F.A., Spaeth, P., Stempien, J.A.,
778 Wang, S.C., 2011. The evolutionary consequences of oxygenic photosynthesis: a body size
779 perspective. *Photosynthesis Research* 107, 37-57.
- 780 Peterson, K.J., Butterfield, N.J., 2005. Origin of the Eumetazoa: Testing ecological
781 predictions of molecular clocks against the Proterozoic fossil record. *Proceedings of the*
782 *National Academy of Sciences of the United States of America* 102, 9547-9552.
- 783 Podkovyrov, V.N., Semikhatov, M.A., Kuznetsov, A.B., Vinogradov, D.P., Kozlov, V.I., Kislova,
784 I.V., 1998. Carbonate carbon isotopic composition in the upper Riphean stratotype, the
785 Karatau group, southern Urals. *Stratigraphy and Geological Correlation* 6, 319-335.
- 786 Pokrovskii, B.G., Melezhik, V.A., Bujakaite, M.I., 2006. Carbon, Oxygen, Strontium and Sulfur
787 isotopic compositions in Late Precambrian Rocks of the Patom Complex, Central Siberia.
788 *Lithology and Mineral Resources*, 450-474.
- 789 Porter, S.M., Meisterfeld, R., Knoll, A.H., 2003. Vase-shaped microfossils from the
790 Neoproterozoic Chuar Group, Grand Canyon: A classification guided by modern testate
791 amoebae. *Journal of Paleontology* 77, 409-429.

- 792 Poulton, S.W., Canfield, D.E., 2005. Development of a sequential extraction procedure for
793 iron: implications for iron partitioning in continentally derived particulates. *Chemical*
794 *Geology* 214, 209-221.
- 795 Poulton, S.W., Canfield, D.E., 2011. Ferruginous Conditions: A Dominant Feature of the
796 Ocean through Earth's History. *Elements* 7, 107-112.
- 797 Poulton, S.W., Fralick, P.W., Canfield, D.E., 2004a. The transition to a sulphidic ocean similar
798 to 1.84 billion years ago. *Nature* 431, 173-177.
- 799 Poulton, S.W., Krom, M.D., Raiswell, R., 2004b. A revised scheme for the reactivity of iron
800 (oxyhydr)oxide minerals towards dissolved sulfide. *Geochimica Et Cosmochimica Acta* 68,
801 3703-3715.
- 802 Poulton, S.W., Raiswell, R., 2002. The low-temperature geochemical cycle of iron: From
803 continental fluxes to marine sediment deposition. *American Journal of Science* 302, 774-
804 805.
- 805 Raaben, M.E., Oparenkova, L.I., 1997. New data on the Riphean stratigraphy of Timan.
806 *Stratigraphy and Geological Correlation* 5, 110-117.
- 807 Raff, R.A., Raff, E.C., 1970. Respiratory mechanisms and metazoan fossil record. *Nature* 228,
808 1003-&.
- 809 Raiswell, R., Buckley, F., Berner, R.A., Anderson, T.F., 1988. Degree of pyritization of iron as
810 a paleoenvironmental indicator of bottom water oxygenation. *Journal of Sedimentary*
811 *Petrology* 58, 812-819.
- 812 Raiswell, R., Canfield, D.E., 1996. Rates of reaction between silicate iron and dissolved
813 sulfide in Peru Margin sediments. *Geochimica Et Cosmochimica Acta* 60, 2777-2787.

- 814 Raiswell, R., Canfield, D.E., 1998. Sources of iron for pyrite formation in marine sediments.
815 *American Journal of Science* 298, 219-245.
- 816 Raiswell, R., Canfield, D.E., Berner, R.A., 1994. A comparison of iron extraction methods for
817 the determination of degree of pyritization and the recognition of iron limited pyrite
818 formation. *Chemical Geology* 111, 101-110.
- 819 Raiswell, R., Newton, R., Wignall, P.B., 2001. An indicator of water-column anoxia:
820 Resolution of biofacies variations in the Kimmeridge Clay (Upper Jurassic, UK). *Journal of*
821 *Sedimentary Research* 71, 286-294.
- 822 Rhoads, D.C., Morse, J.W., 1971. Evolutionary and ecologic significance of oxygen deficient
823 marine basins. *Lethaia* 4, 413-&.
- 824 Ries, J.B., Fike, D.A., Pratt, L.M., Lyons, T.W., Grotzinger, J.P., 2009. Superheavy pyrite (δ
825 $S-34(\text{pyr}) > \delta S-34(\text{CAS})$) in the terminal Proterozoic Nama Group, southern Namibia: A
826 consequence of low seawater sulfate at the dawn of animal life. *Geology* 37, 743-746.
- 827 Rothman, D.H., Forney, D.C., 2007. Physical model for the decay and preservation of marine
828 organic carbon. *Science* 316, 1325-1328.
- 829 Runnegar, B., 1991. Precambrian oxygen levels estimated from the biochemistry and
830 physiology of early eukaryotes. *Palaeogeography Palaeoclimatology Palaeoecology* 97, 97-
831 111.
- 832 Scott, C., Lyons, T.W., Bekker, A., Shen, Y., Poulton, S.W., Chu, X., Anbar, A.D., 2008. Tracing
833 the stepwise oxygenation of the Proterozoic ocean. *Nature* 452, 456-U455.
- 834 Seibel, B.A., Drazen, J.C., 2007. The rate of metabolism in marine animals: environmental
835 constraints, ecological demands and energetic opportunities. *Philosophical Transactions of*
836 *the Royal Society B-Biological Sciences* 362, 2061-2078.

- 837 Sergeev, V.N., Precambrian microfossils in cherts: their paleobiology, classification, and
838 biostratigraphic usefulness. GEOS, Moscow, p. 280.
- 839 Sergeev, V.N., 2006. Precambrian microfossils in cherts: their paleobiology, classification,
840 and biostratigraphic usefulness. GEOS, Moscow, p. 280.
- 841 Sergeev, V.N., Knoll, A.H., Vorob'eva, N.G., 2011. Ediacaran microfossils from the Ura
842 Formation, Baikal-Patom uplift, Siberia: Taxonomy and Biostratigraphic significance.
843 *Journal of Paleontology* 85, 987-1011.
- 844 Sergeev, V.N., Seong-Joo, L., 2006. Real eukaryotes and precipitates first found in the Middle
845 Riphean stratotype, southern Urals. *Stratigraphy and Geological Correlation* 14, 1-18.
- 846 Severmann, S., Lyons, T.W., Anbar, A., McManus, J., Gordon, G., 2008. Modern iron isotope
847 perspective on the benthic iron shuttle and the redox evolution of ancient oceans. *Geology*
848 36, 487-490.
- 849 Shen, Y.N., Zhang, T.G., Hoffman, P.F., 2008. On the coevolution of Ediacaran oceans and
850 animals. *Proceedings of the National Academy of Sciences of the United States of America*
851 105, 7376-7381.
- 852 Sokolov, B.S., Fedonkin, M.A., 1990. *The Vendian System*. Springer-Verlag, Berlin.
- 853 Sokolov, B.S., Iwanowski, A.B., 1990. *The Vendian System: Paleontology, The Vendian*
854 *System*. Springer-Verlag, Berlin.
- 855 Sperling, E.A., Vinther, J., 2010. A placozoan affinity for Dickinsonia and the evolution of late
856 Proterozoic metazoan feeding modes. *Evolution & Development* 12, 201-209.
- 857 Stanley, S.M., 1973. Ecological theory for sudden origin of multicellular life in late
858 Precambrian. *Proceedings of the National Academy of Sciences of the United States of*
859 *America* 70, 1486-1489.

- 860 Swanson-Hysell, N.L., Rose, C.V., Calmet, C.C., Halverson, G.P., Hurtgen, M.T., Maloof, A.C.,
861 2010. Cryogenian Glaciation and the Onset of Carbon-Isotope Decoupling. *Science* 328, 608-
862 611.
- 863 Tosca, N.J., Johnston, D.T., Mushegian, A., Rothman, D.H., Summons, R.E., Knoll, A.H., 2010.
864 Clay mineralogy, organic carbon burial, and redox evolution in Proterozoic oceans.
865 *Geochimica Et Cosmochimica Acta* 74, 1579-1592.
- 866 Turekian, K.K., Wedepohl, K.H., 1961. Distribution of the elements in some major units of
867 the Earth's crust. *Geological Society of America Bulletin* 72, 175-191.
- 868 Vaquer-Sunyer, R., Duarte, C.M., 2008. Thresholds of hypoxia for marine biodiversity.
869 *Proceedings of the National Academy of Sciences of the United States of America* 105,
870 15452-15457.
- 871 Vorob'eva, N.G., Sergeev, V.N., Knoll, A.H., 2009a. Neoproterozoic microfossils from the
872 margin of the East European Platform and the search for a biostratigraphic model of lower
873 Ediacaran rocks. *Precambrian Research* 173, 163-169.
- 874 Vorob'eva, N.G., Sergeev, V.N., Knoll, A.H., 2009b. Neoproterozoic microfossils from the
875 northeastern margin of the East European Platform. *Journal of Paleontology* 83, 161-196.
- 876 Yin, L.M., Zhu, M.Y., Knoll, A.H., Yuan, X.L., Zhang, J.M., Hu, J., 2007. Doushantuo embryos
877 preserved inside diapause egg cysts. *Nature* 446, 661-663.
- 878 Yuan, X.L., Chen, Z., Xiao, S.H., Zhou, C.M., Hua, H., 2011. An early Ediacaran assemblage of
879 macroscopic and morphologically differentiated eukaryotes. *Nature* 470, 389-392.
- 880
- 881



HARVARD UNIVERSITY
DEPARTMENT OF EARTH AND PLANETARY SCIENCES
20 OXFORD ST.
CAMBRIDGE, MA 02138
TEL. (617) 495-2351 FAX. (617) 495-8839

Highlights for *Late Ediacaran redox stability and metazoan evolution* by Johnston *et al.*

- 1) Redox stability, in addition to O₂, is critical for animal evolution.
- 2) We explain Ediacaran global asynchronicity in sedimentary proxy and animals records.
- 3) We revisit the importance of dysoxia for biological evolution.
- 4) The data reinforce that Ediacaran acritarchs are resting stages of early animals.